Carbohydrate Polymers 101 (2014) 828–836

Contents lists available at ScienceDirect

Carbohydrate Polymers

journal homepage: www.elsevier.com/locate/carbpol

Inclusion complex of sulfadimethoxine with cyclodextrins: Preparation and characterization

N. Rajendiran*, S. Siva

Department of Chemistry, Annamalai University, Annamalai nagar 608 002, Tamilnadu, India

ARTICLE INFO

Article history:
Received 10 June 2013
Received in revised form 23 August 2013
Accepted 4 October 2013
Available online 12 October 2013

Keywords:
Sulfadimethoxine
Cyclodextrins
Inclusion complexation
Nanoparticles
Molecular modeling

ABSTRACT

The inclusion complexation behavior, characterization and binding ability of sulfadimethoxine (SDMO) with α-cyclodextrin (α-CD) and β-cyclodextrin (β-CD) have been investigated both in solution and solid state by means of absorption, fluorescence, time-resolved fluorescence, ^{1}H NMR, FT-IR, DSC, SEM, TEM, XRD and molecular modeling methods. The spectral shifts revealed that the part of pyrimidine and aniline rings of SDMO are entrapped in the CD cavity. The stoichiometric ratio and association constant were determined by Benesi–Hildebrand plots and spectroscopic studies respectively. FT-IR spectroscopy was used to compare inclusion systems with physical mixtures, and demonstrated the complex formation in the solid state. The morphology and size of the nanoparticles of SDMO/CD complexes in aqueous solution were observed by TEM. The DSC analysis showed that the thermal stability of SDMO was enhanced in the presence of CD. Investigations of energetic and thermodynamic properties by PM3 method confirmed the stability of the inclusion complexes.

1. Introduction

Sulfonamides have been extensively used in pharmaceuticals for the treatment of human and farm animal infectious diseases caused by gram-positive and gram-negative microorganisms and fungi (Perez-Trallero & Iglesias, 2003; Schmitt, Haapakangas, & van Beelen, 2005). Sulfadimethoxine (4-amino-*N*-(2,6-dimethoxy-4-pyrimidynyl)benzenesulfonamide, SDMO), is one of the synthetic anti-microbial having the bioactive *p*-amino group, generally administered via food to farm animals such as hen, cow, etc., for the prevention of bacterial infections and coccidiosis with a broad spectrum activity. Even though, the over drug dosages of SDMO in animal foods is of great anxiety, because it can produce residue that present in marketed milk, egg and chicken meat (Kishida & Furusawa, 2005). European Union (EU) and Republic of Korea have set maximum residue limit up to 100 $\mu g\,kg^{-1}$ and 10 $\mu g\,kg^{-1}$ respectively, for SDMO in foods of animal origin to assure the food safety for consumers (Chung, Lee, Chung, & Lee, 2009). Most of the antibiotics are poorly absorbed by human and farm animals after intake due to their poor bioavailability. The oral bioavailability of SDMO is laid between 25% and 70% (Yu et al., 2011). Thus, it is more essential to search for an efficient and non-toxic carrier for SDMO to extend its therapeutic applications. The solubility of poorly water soluble drug can be increased by utilizing several ways, such as modification of drug crystal forms, addition of cosolvents, addition of surfactants, addition of cyclodextrins (CDs), etc. Among the different ways to overcome the poor solubility, the molecular encapsulation of the drug by CDs is of great concern.

CDs are non-toxic, macrocyclic oligosaccharides, consisting of six or more α-1,4-linked D-glucopyranose units. They have a hydrophobic central cavity and hydrophilic outer surface and can encapsulate model substrates to form host-guest complexes of supramolecular species. Among these CDs, α-, β- and γ-CD are most frequently used and studied for dissolution rate enhancement (Inoue et al., 1993a). They have the property of forming inclusion complexes with various guest molecules of suitable polarity and dimension because of their truncated-cone molecular structure (Connors, 1997). Inclusion complexes of CDs are being formulated and studied for varied purposes such as dissolution rate enhancement, solubility of the poorly water soluble drugs, stability of the system and even as drug carriers (Fernandez et al., 2008; Carrier, Miller, & Ahmed, 2007). Thus CDs have been widely used in pharmaceutical industry, foods, separation techniques and environmental protection (Loftsson & Duchene, 2007; Szejtli, 1998).

In our previous studies, a sequence of sulfonamide derivatives with β-CD were investigated through experimental (Premakumari et al., 2011; Prabhu, Venkatesh, & Rajendiran, 2010) and theoretical methods (Venkatesh, Sivasankar, Karthick, & Rajendiran, 2013). The study in aqueous solution clearly demonstrated that the presence of intramolecular charge transfer (ICT) or twisted intramolecular charge transfer (TICT) in the first excited state as evidenced by the appearance of large Stokes shifted longer

* Corresponding author. Tel.: +91 94866 28800; fax: +91 4144 238080.
E-mail address: drrajendiran@rediffmail.com (N. Rajendiran).

0144-8617/$ – see front matter © 2013 Elsevier Ltd. All rights reserved.
http://dx.doi.org/10.1016/j.carbpol.2013.10.016

wavelength (LW) emission. The increased emission intensity of LW with a considerable bathochromic shift in CD solution has been attributed to the enhancement of TICT in these sulfanilamide molecules. PM3 calculation has been applied on the large molecular inclusion complex systems. This calculation suggested that the inclusion complexation process was spontaneous and enthalpy driven. Further the combination of experimental and theoretical work leads to successful results in solving structural, energetic and dynamic problems (Sivasankar, Prabhu, Karthick, & Rajendiran, 2012; Prabhu, Sankaranarayanan, Venkatesh, & Rajendiran, 2012). In addition, Longhi and coworkers (Garnero, Aiassa, & Longhi, 2012; Delrivo, Zoppi, & Longhi, 2012) studied the inclusion complexes of sulfamethoxazole and sulfadiazine with β-cyclodextrin and its derivatives in aqueous solution and in solid state. However, no reports about the characterization of the new systems (SDMO/CD) in solution or in solid state have been published.

Herein we report the preparation and characterization of inclusion complexes formed by SDMO with α- and β-CD. We utilized absorption and fluorescence spectral titration techniques to determine the inclusion stoichiometry and association constant of SDMO/CD complexes, and characterized the solid inclusion complexes by ^{1}H NMR, FT-IR, differential scanning calorimetry (DSC), scanning electron microscopy (SEM), transmission electron microscopy (TEM) and powder X-ray diffraction (XRD) methods. PM3 method was also applied to study the inclusion process of the drug within CDs and the minimum energy structures of 1:1 inclusion complexes were proposed.

2. Materials and methods

2.1. Materials

Sulfadimethoxine (SDMO, 98.5%), α-CD (98%) and β-CD (98%) were purchased from Sigma–Aldrich chemical company and used as such. All other chemicals and solvents used were of the highest grade (Spectrograde) commercially available. Triply distilled water was used for the preparation of aqueous solutions. The aqueous solutions were prepared just before each measurement. Purity of the drug was checked by melting point and also by fluorescence techniques, i.e., by getting same spectral profile when excited with different wavelengths.

2.2. Preparation of inclusion complexes in solutions

A serious of samples with constant concentration of SDMO drug and different concentrations of α-CD and β-CD were prepared. The concentration of the drug solutions was maintained at 4×10^{-5} M and the CD concentrations were varied from 1.0×10^{-3} to 1.0×10^{-2} M. The mixture of drug-CD solutions were shaken thoroughly and kept for 6 h to bring them to a state of equilibrium. The experiments were carried out at room temperature (30 °C).

2.3. Preparation of inclusion complexes in solid state

The solid inclusion complexes were prepared by coprecipitation method. The α-CD or β-CD (0.973 or 1.14 g) was dissolved in 40 ml distilled water at 40 °C in a water bath. The drug (0.310 g) in 10 ml methanol was slowly added to the CD solution with continuous agitation. The molar ratio of drug to CD was 1:1. The vessel was covered with aluminum foil and stirred continuously for 24 h at room temperature and the solution was refrigerated overnight at 5 °C. The precipitated drug-CD inclusion complexes were recovered by filtration and washed with minimum amount of methanol and water to remove uncomplexed drug and CD respectively. The precipitate was then dried in vacuum at room temperature for two days and stored in an airtight bottle.

2.4. Instruments

Absorption and fluorescence spectral measurements were carried out with Shimadzu UV–visible spectrophotometer (model 1650 PC) and Shimadzu spectrofluorimeter (model RF-5301) respectively. Fluorescence lifetime measurements were performed using a pico-second laser and a single-photon counting setup from Jobin-Yvon IBH (Madras University, Chennai, India). The fluorescence decay of the sample was analyzed using IBH data analysis software. One-dimensional ^{1}H NMR spectra for drug and its CD inclusion complexes were recorded on a Bruker AVANCE 500 MHz spectrometer (Germany) using an inverse broadband (BBI) probe at room temperature. Samples were dissolved in DMSO-d_6 (99.98%) and were equilibrated for at least 1 h. FT-IR spectra of powder sample of drug, CD and the inclusion complexes were measured between 4000 cm^{-1} and 400 cm^{-1} on a JASCO FT-IR-5300 spectrometer using KBr pellet with 256 scans at a resolution of 4 cm^{-1}. Thermal characteristics of solid inclusion complexes were measured using Mettler Toledo DSC1 fitted with STR^e software (Mettler Toledo, Switzerland), temperature scanning range was from 25 to 220 °C with a heating rate of 10 °C/min. Microscopic morphological structures of the raw materials and the inclusion complexes were investigated and photographed using a scanning electron microscope (Hitachi S3400N). The morphological structures of drug-encapsulated complexes (SDMO/α-CD and SMDO/β-CD) were investigated by TEM using TECNAI G^4 microscope with an accelerating voltage of 200 kV. XRD patterns of powder samples were recorded using a BRUKER D8 Advance diffractometer (Bruker AXS GmbH, Karlsruhe, Germany) with Cu KαI radiation (λ = 1.5406 Å), with the voltage of 40 kV and 20 mA current.

2.5. Molecular modeling

The theoretical calculations were performed using Gaussian 03 W package. The initial geometry of SDMO, α-CD and β-CD were constructed with Spartan 08 and then fully optimized by PM3 method without any symmetry constraint. The inclusion complexes were constructed from the PM3 optimized CD and guest molecules. The longer dimension of the guest molecule was initially placed onto the *Z* axis. The position of the guest was determined by the Z coordinate of one selected atom of the guest. Complete geometry optimizations without any restriction with PM3 method were employed in the study of the complexation process of the drug within α-CD and β-CD. The most energetically favorable structures of the drug as well as CD molecules were used to construct CD inclusion complexes. These drug-CD complexes were constructed manually by inserting the drug into the CD cavity through the wider rim, centering it on a vector perpendicular to the mean plane through the glycosidic oxygen atoms.

3. Results and discussion

3.1. Absorption spectral characteristics of SDMO in CDs

Spectrophotometric and fluorimetric titrations were done to determine the molecular encapsulation behavior of α-CD and β-CD with SDMO in aqueous solution. It has been observed that the shape, position of peak maximum and molar absorption coefficient of the drug molecule strongly depends on the CD cavity environments. Fig. 1a and b displays the absorption spectra of the drug as a function of α-CD and β-CD concentrations at pH ~ 6.5. The absorption spectrum of the drug itself in aqueous solution exhibits

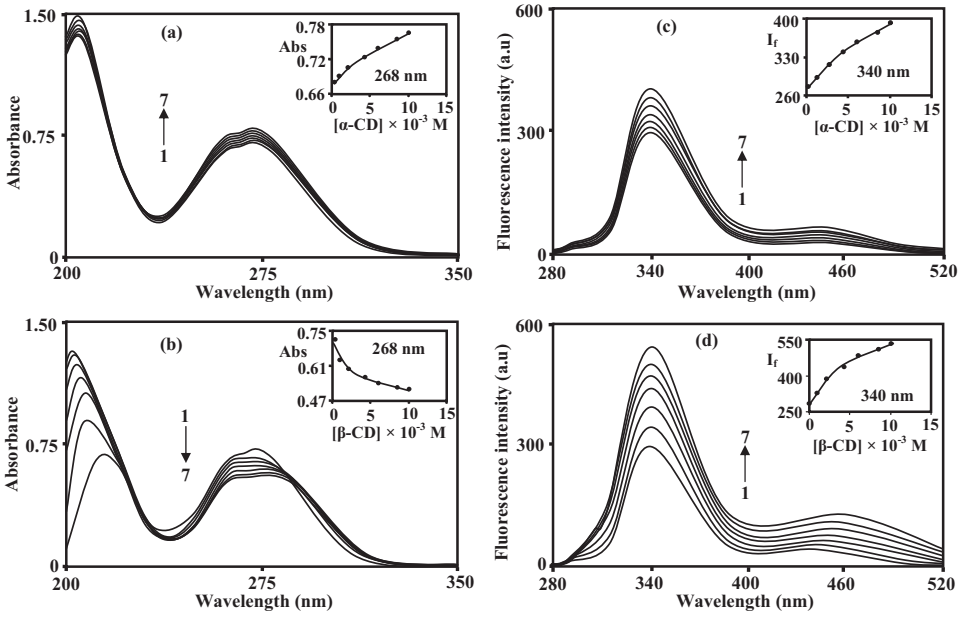

Fig. 1. (a and b) Absorption and (c and d) fluorescence spectra of SDMO in different α-CD and β-CD concentrations (M): (1) 0, (2) 0.001, (3) 0.002, (4) 0.004, (5) 0.006, (6) 0.008 and (7) 0.01. Inset figures: intensity versus CD concentration.

a single absorption maximum at ~268 nm. Upon the addition of β-CD, the absorption maxima of SDMO are red shifted about ~5 nm with a gradual decrease in absorbance. Whereas there is no remarkable spectral shift was noticed in the presence of α-CD except an increase in the intensity. The above spectral changes might suggest that the strong interactions between the drug and CDs. However, the red shift observed in β-CD solutions was caused as a result of decreasing polarity of the CD cavity environment experienced by the drug molecule. Further, the decrease or increase of absorbance in CD solutions has been attributed to the enhanced dissolution of the drug through the hydrophobic interaction of CD cavity (Siva, Thulasidhasan, & Rajendiran, 2013).

3.2. Fluorescence spectral studies

The fluorescence emission spectra of SDMO in aqueous solution containing various concentrations of α-CD and β-CD are shown in Fig. 1c and d. The effect of CDs on the emission spectra of the drug molecule are more pronounced than the corresponding effect on the absorption spectra with respect to the concentration of CDs. The maximum excitation and emission wavelengths were 270 and 339, 438 nm respectively. It has been reported earlier (Premakumari et al., 2011) that sulfonamide derivatives undergo normal as well as highly Stokes shifted fluorescence. The normal fluorescence takes place from the locally excited (LE) state while the twisted intramolecular charge transfer (TICT) is responsible for highly Stokes shifted fluorescence. It can be seen from Fig. 1 that the LE emission intensity is greater than that of TICT emission intensity. It is noteworthy that with increasing concentrations of β-CD, a regular red shift was observed in the TICT emission (about ~8 nm), whereas no considerable change was observed in the LE emission. While the fluorescence intensities of both emissions were enhanced at the same wavelengths with increasing concentrations of α-CD. Thus, it can be suggested that the spectral shift might be corresponding to energy stabilization of the emitting state and characteristic for the fluorescence of TICT state. These data suggested that the strong interactions between SDMO and CDs, and the formation of stable inclusion complexes. The enhancement of the fluorescence intensity of both LE and TICT emission bands may be due to lowering of solvent polarity provided by CD cavity and the non-radiative path of LE emission is restricted through TICT state. Further, the enhancement of TICT emission is observed in both CDs suggesting that the inclusion process plays a major role in the TICT emission. This inference is supported by similar emission spectra observed when excited CD solutions containing sulfa drug with different emission wavelengths at ~340 and 440 nm, respectively.

Naturally two different types of inclusion complex formation are possible: (i) the pyrimidine ring encapsulated in the CD cavity and (ii) the aniline ring encapsulated in the CD cavity. If the pyrimidine ring is included in to the CD cavity, the monocation maxima of the sulfonamide molecule (protonation of tertiary nitrogen atom) should be red shifted in CD than aqueous medium. The red shift in β-CD solution indicates that the heterocyclic ring interacts with CD hydroxyl groups. Moreover, in this complex, the CD cavity will impose a restriction on the free rotation of the $-OCH_3$ group or pyrimidine group in its excited state and TICT emission should increase in CD medium. These features support the idea that the TICT state in CD is stabilized through complexation. This confirms that the environments around the amino group in CD medium are same as in the bulk aqueous medium. The above results suggest that a part of aniline and pyrimidine ring is present into the center of the CD cavity.

3.3. Determination of stoichiometry and association constant

The stoichiometric ratio and association constant (K) for the formation of drug/CD complexes have been determined by analyzing the changes in the intensity of absorption and emission maxima with the CD concentrations. The stoichiometric ratio and association constant (K) of the inclusion complexes of SDMO can be determined according to modified Benesi and Hildebrand (1949) (B–H) equation.

$$\frac{1}{(I - I_0)} = \frac{1}{\alpha} + \frac{1}{(\alpha K[CDs])} \quad (1)$$

where, I_0 and I are the absorption/emission intensities of SDMO in the absence and in the presence of CDS, respectively; K is the association constant and α is a constant.

The stoichiometric ratio of SDMO/CD complexes was estimated from the B–H double-reciprocal plots. Typical double-reciprocal

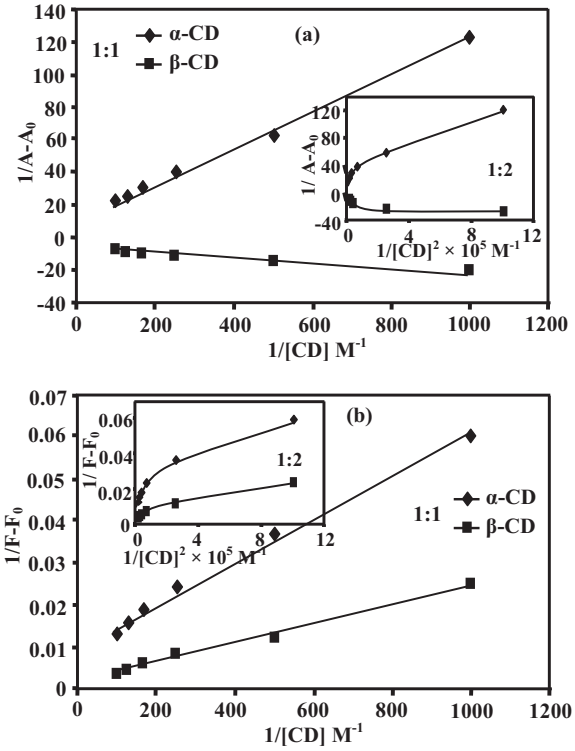

Fig. 2. Double reciprocal plots for 1:1 complexation of SDMO with α-/β-CD obtained from (a) absorption and (b) fluorescence data. Inset figures: double reciprocal plots for 1:2 complexation.

plots for the studied complexes are shown in Fig. 2. A good linear relationship is obtained when $1/(I–I_0)$ is plotted against 1/[CDs], indicating that the stoichiometry of the complexes is 1:1. The association constant (K) for the inclusion complex formation obtained from the slope and intercept of the B–H plots was found to be SDMO/α-CD ≈ abs = 216 M^{-1}, flu = 347 M^{-1} and SDMO/β-CD ≈ abs = 284 M^{-1}, flu = 863 M^{-1}. The variation in the association constants suggested that the inclusion capability of CDs with guest molecule. In other words the β-CD has greater inclusion ability than α-CD. Moreover, the plot of $1/(I–I_0)$ versus $1/[CDs]^2$ gives an upward and/or downward curves (Inset in Fig. 2). The nonlinearity of the plots ruled out the possibility of 1:2 stoichiometry between the drug molecule and CDs. Thus, we have concluded that the stoichiometry of the inclusion complexes was 1:1 as evidenced by fitting a double-reciprocal plot of $1/(I–I_0)$ versus 1/[CDs].

The thermodynamic parameter, Gibbs free energy change (ΔG) for the binding of guest molecules within α-CD (abs = −3.23, flu = −3.52 kcal/mol) and β-CD (abs = −3.40, flu = −4.07 kcal/mol) were determined. The negative ΔG values of the complexes suggest that the binding process is spontaneous and thermodynamically favored in the experimental temperature range. The hydrophobic interaction between the internal wall of CD and guest molecules is an important factor for the stability of the inclusion complexes. In the case of SDMO/α-CD and SDMO/β-CD, it may safely be considered that the difference in the magnitude of the hydrophobic interaction is allied to the contact area of the guest molecule and the internal wall of CD.

3.4. Time-resolved fluorescence analysis

The fluorescence lifetime decay curves of SDMO in water, α-CD and β-CD (0.01 M) have been measured. The fluorescence decay curve for the free drug (SDMO) in water was fitted to biexponential function with χ^2 values of ∼1.1 in the absence of CDs. This indicates that the drug has two lifetime components: One causative maximum of the total fluorescence (τ_1 = 0.29 ns) and the other causative is the rest of fluorescence (τ_2 = 3.28 ns). The first with a longer lifetime is assigned to LE emission and the other to TICT state of guest molecule. It is noteworthy that the decay time of the slow component is different to that of TICT emission within experimental uncertainty. This indicates that a little equilibrium between the LE state and the TICT state is achieved in water rather in a short period. By the addition of CDs, biexponential decay curve becomes triexponential. Three lifetimes >(τ_1 = 0.43/0.55 ns, τ_2 = 1.14/1.89 ns and τ_3 = 4.83/5.58 ns) were obtained in the presence of both α-CD and β-CD. The above data reflect that the observed lifetime values increase with the addition of CD concentration in aqueous solution, due to the inclusion complex formation between the drug and CDs. The observed enhancement in lifetime indicates that SDMO molecule experiences less polar hydrophobic environments within the CD cavity resulting in the reduction of non-radiative decay processes. Further, the increase in fluorescence lifetime is a result of the significant interactions of the sulfa drugs with hydrophobic CD cavity. The efficient lifetime enhancement is found to be higher with β-CD, which reveals the stronger hydrophobic interaction between the SDMO and β-CD.

3.5. Characterization of solid inclusion complexes

3.5.1. ^{1}H NMR spectral studies

A direct evidence for the complexation of SDMO with CDs and the possible inclusion mode of the inclusion complexes can be obtained from ^{1}H NMR spectroscopy, which has been proved to be a useful analytical tool in the study of CD inclusion complexes (Lehman & Klienpeter, 1991). In this study, ^{1}H NMR spectroscopy provides an effective means of evaluating the interaction mode of CD with that of the sulfa drug. The information obtained from ^{1}H NMR spectroscopy is the chemical shift displacement, loss of resolution and broadening of selective signals of the host and guest protons. Fig. S1a (see Supplementary data) displays the ^{1}H NMR spectrum of SDMO drug and the assignment of signals. The spectral data for pure SDMO and the drug in α-/β-CD complexes (in parenthesis) are as follows: H_a ∼ 11.105 (11.084/11.077), H_b ∼ 7.552 (7.526/7.523), H_c ∼ 6.590 (6.552/6.547), H_d ∼ 6.097 (6.082/6.081), H_e ∼ 5.919 (5.905/5.902), H_f ∼ 3.778 (*), H_g ∼ 3.771 (*). It can be seen from the above data that H_a, H_b, H_c, H_d, and H_e protons of SDMO showed larger chemical shift changes by about 0.014–0.032 ppm, because of the diminished freedom of rotation caused by the insertion of the SDMO molecule into the CD cavity. This reveals that a part of the aniline moiety and pyrimidine ring were entered into the center of CD cavity. However, the chemical shift change values for H_f and H_g protons could not be determined due to the merging of these signals with that of CDs.

To further explore the inclusion mode, the chemical shifts of CD protons in the absence and in the presence of SDMO were investigated. The resonance assignments of the CD protons are well established and consist of six types of protons. The chemical shift of CD protons reported by different authors are very close to those reported in this work. The insertion of SDMO into the CD cavity caused an upfield shift of CD protons. As can be seen from Fig. S1, inclusion complexation with the sulfa drug had a negligible effect on the δ values of H-1, H-2, H-4 and H-6 protons of CD (∼0.007 ppm). In contrast, those values of H-3 and H-5 protons which are located in the interior of the cavity exhibited significant changes (∼0.032–0.048 ppm). It is fairly noteworthy that H-3 protons shifted about ∼0.048 ppm, but H-5 protons showed weak shifts (∼0.032 ppm) after the formation of inclusion complexes. Because both H-3 and H-5 protons are located in the interior of CD cavity, and H-3 protons are nearer to the wider side of cavity while H-5 protons are nearer to the narrow side, this phenomenon may

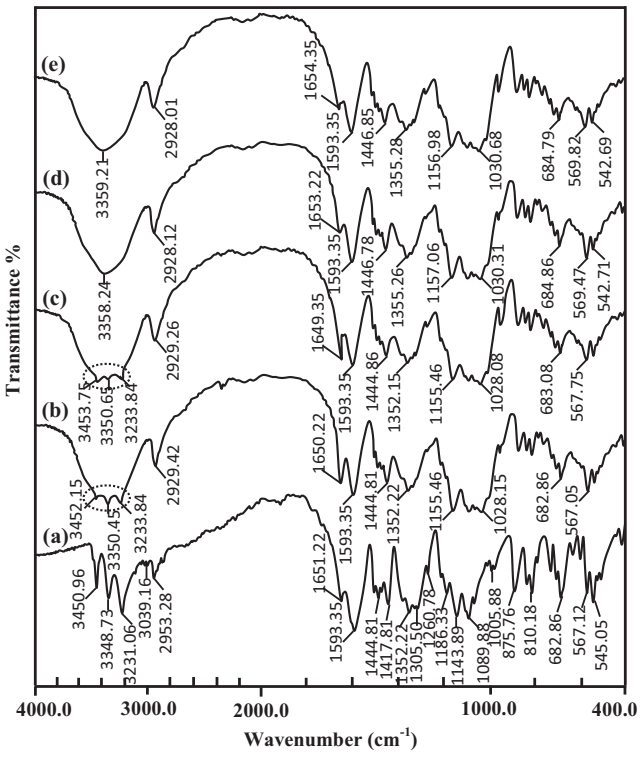

Fig. 3. FT-IR spectra of (a) SDMO, (b) SDMO/α-CD physical mixture, (c) SDMO/β-CD physical mixture, (d) SDMO/α-CD complex and (e) SDMO/β-CD complex.

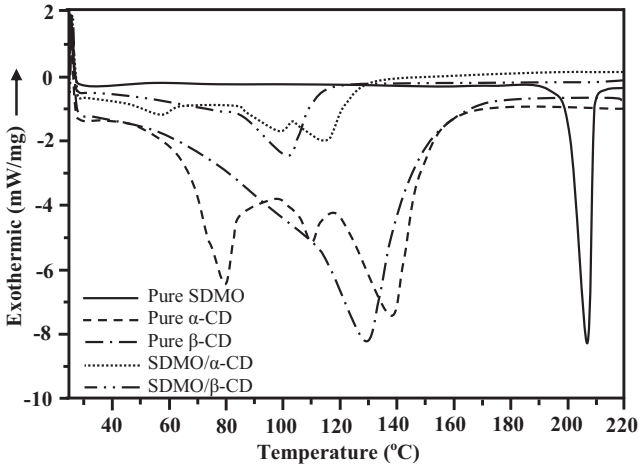

Fig. 4. DSC curves of (a) SDMO, (b) α-CD, (c) β-CD, (d) SDMO/α-CD complex and (e) SDMO/β-CD complex (25–220 °C at 10 °C/min).

indicate that the aniline moiety of SDMO should penetrate into the CD cavity from the wider rim side.

3.5.2. FT-IR spectroscopy

The encapsulation of SDMO into CD cavity was confirmed by FT-IR spectroscopy because the bands resulting from the inserted part of the guest molecule are generally shifted or their intensities changed. FT-IR spectra of SDMO, α-CD, β-CD, physical mixture and the inclusion complexes are presented in Fig. 3. The IR spectrum of the drug (Fig. 3a) was characterized by principal absorption peaks at 3450 and 3348 cm^{-1} (for NH stretching in SO_2—NH group), 3231 cm^{-1} (for NH_2 stretching), 1651 cm^{-1} (for NH_2 deformation), 1593 cm^{-1} (for C=C stretching), 1444 and 1352 cm^{-1} (for CH_3 deformation), 1305 cm^{-1} (for SO_2 asymmetric stretching), 1260 cm^{-1} (for C—O stretching in —$COCH_3$ group), 1186 cm^{-1} (for SO_2 symmetric stretching), 1089 and 810 cm^{-1} (for C—H deformation in phenyl ring), 1005 cm^{-1} (for C—N stretching), 875 cm^{-1} (for S—N stretching) and 545 cm^{-1} (for SO_2 deformation), which are in agreement with the FT-IR spectrum corresponding to SDMO reported by Ulusoy, Topacli, and Ide (1998). The FT-IR spectra of CD consists of the prominent absorption peaks of O—H stretching (3392 cm^{-1}), C—H stretching (2926 cm^{-1}), H—O—H bending (1646 cm^{-1}), C—O stretching (1157 cm^{-1}) and C—O—C bending (1028 cm^{-1}). It can be seen that in the FT-IR spectra of the physical mixture (Fig. 3b and c), there were no changes since they were derived from the superimposition of the spectra of the single components, suggesting the absence of interactions. In these spectra the NH and NH_2 stretching frequencies of SDMO were masked by huge number of OH groups of α-/β-CD (showed as dotted circle in Fig. 3b and c). Similar results have been observed by other researchers for the physical mixtures of sulfamethoxazole and sulfadiazine with β-CD (Garnero et al., 2012; Delrivo et al., 2012). In contrast, the IR spectral features of the pure drug were completely disappeared in the inclusion complexes (Fig. 3d and e). The band assigned to the NH in SO_2—NH group and NH_2 stretching was completely disappeared in the inclusion complexes. The bands positioned at ~1651, 1593, 1260–1089 cm^{-1} were shifted and their intensities were diminished. The NH_2 deformation and CH_3 deformation frequencies were shifted in the inclusion complexes to 1654 and 1446, 1355 cm^{-1} respectively. However, the C—N stretching was shifted to lower frequency (992 cm^{-1}) in the inclusion complexes. The S—N stretching and SO_2 deformation bands became shorter and shifted to lower frequencies of 871 and 542 cm^{-1}, respectively. The above changes can be due to the formation of SDMO/CD inclusion complexes in solid state. According to the above FT-IR analysis of inclusion complexes, we might suggest that the aniline ring of the SDMO was involved in the complexation and the amino group is present outside of the CD cavity. Nevertheless, no new chemical bonds were formed, reveals that the non-covalent interactions between the drug and CDs. These results may be due to the presence of van der Waals interactions between CD and SDMO. In this regard, van der Waals interactions are generally considered to contribute to the formation of inclusion complexes with CDs.

3.5.3. Differential scanning calorimetry (DSC)

DSC represents an effective and inexpensive analytical tool for an accurate physicochemical characterization of encapsulation (drug-CD) systems in the solid state and is widely used for a rapid preliminary qualitative investigation of the thermal behavior of the isolated components and the inclusion complexes prepared according to a standard procedure such as coprecipitation (Kacso, Borodi, Farcas, Hernanz, & Bratu, 2010). The DSC thermograms of pure drug, α-CD, β-CD and their inclusion complexes are displayed in Fig. 4, as comparatively. The thermal curve of SDMO was typical of a crystalline anhydrous substance with a sharp endothermic peak at ~207 °C indicating the melting point of the drug. The DSC profile of α-CD showed three endothermic peaks around at ~79, 109, 137 °C and a broad endothermic peak at ~128 °C was observed for β-CD. These endothermic peaks are mostly associated to crystal water losses from CD cavities. However, the complete disappearance of characteristic melting peak of SDMO in the DSC curves of the solid inclusion systems is an indicative of molecular encapsulation of the drug inside the CD cavity. The characteristic endothermic peaks corresponding to the free α- and β-CD were shifted to ~58, 100, 115 °C and 103 °C respectively, accompanied by significant decrease in the intensity. These findings revealed that the formation of inclusion complexes of CDs with the guest in solid dispersion and/or inclusion complexes with different properties. The shifts of thermal features of CDs and reduced peak intensity could be the evidence for the replacement of water by drug due to

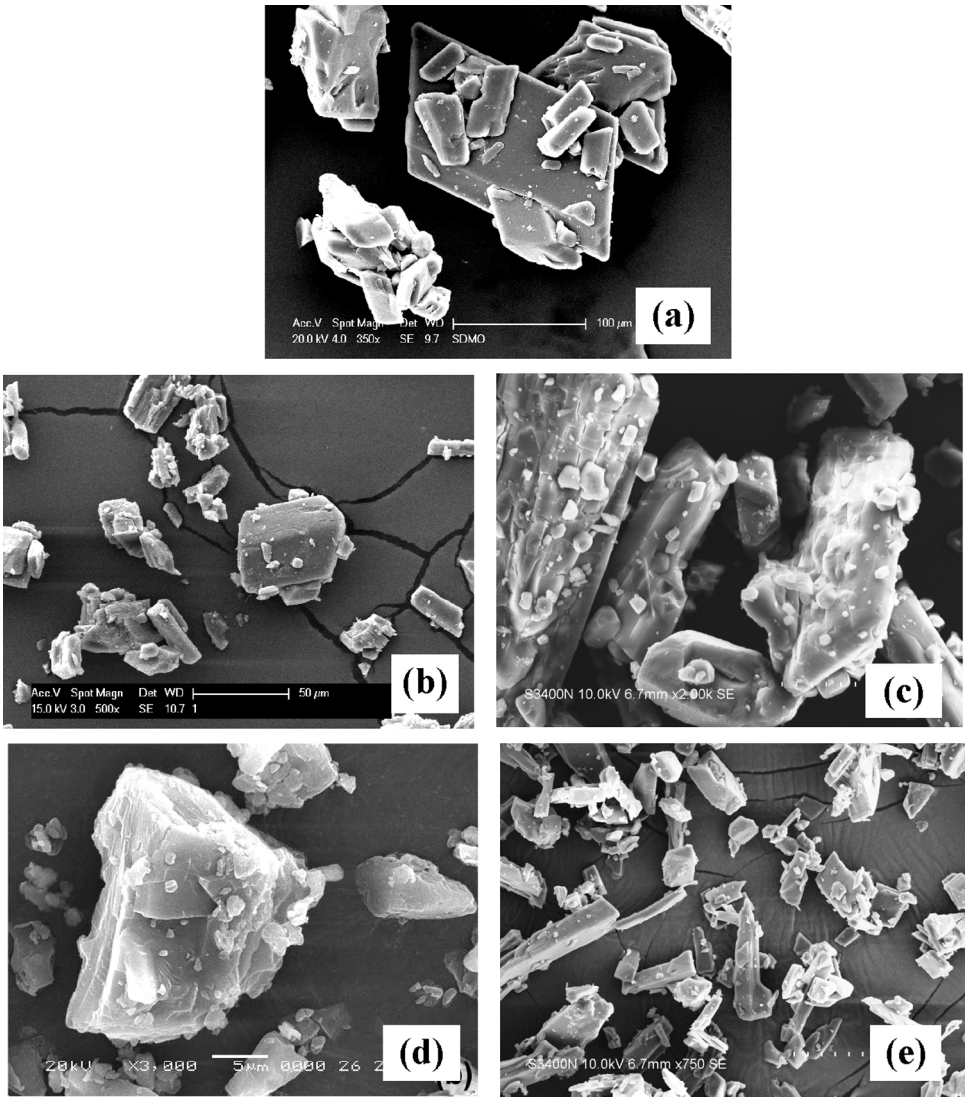

Fig. 5. SEM photographs of (a) SDMO, (b) α-CD, (c) SDMO/α-CD complex, (d) β-CD (e) SDMO/β-CD complex.

complex formation. Similar reduction in maximum dehydration peak was also observed by Hadaruga and coworkers (Hadaruga et al., 2006) after complex formation. Further the second scans in DSC thermograms in the region 40–140 °C without appearance of any peak confirms that the endothermic peaks appearing in this area at the first scans were due to evaporation of water and drug. The DSC data indicated that usual thermal properties of the drug as well as the isolated CDs were altered during inclusion complex formation.

3.5.4. Scanning electron microscopy (SEM)

The surface morphology and size of the pure materials and the changes produced on inclusion complexes were analyzed by SEM. Fig. 5 illustrates the SEM images of solid complexes along with the pure components, i.e., SDMO, α-CD and β-CD. These images were utilized to evaluate the effect of coprecipitation process on the morphology of the solids used for the formation of solid systems. The SEM photographs clearly elucidate the difference between the pure components and their inclusion complexes. It can be seen in SEM images that the SDMO crystals are in the form of sheets with smooth surface. Pure α-CD particles existed in prismatic shape with well-developed faces and β-CD was observed as plate shaped crystals. In contrast, the SDMO/α-CD samples were appeared in irregular shapes with variable size whereas a bar like shape was observed for SDMO/β-CD complex. Furthermore, the size and shape of the SDMO and CDs were different from those of the solid complexes in which the actual morphology of both pure components disappeared. These changes can be taken as a proof for the formation of new inclusion complexes by molecular encapsulation.

3.5.5. Transmission electron microscopy (TEM)

TEM is a more reliable analytical tool in order to investigate the nano-structural features of the wall of the CD encapsulated sulfa drug in aqueous solution (Li & Mcgown, 1994; Sun et al., 2011). The molecular encapsulations of the drug within the CD cavity are reflected in TEM images as shown in Fig. 6. The images show well-ordered zero-dimensional (0D) nano sized particles for both inclusion complexes. In the case of SDMO/α-CD complex, the particles were obtained in the range of 90, 95 and 110 nm at higher magnification in TEM. In β-CD complex, the nanoparticles were highly agglomerated (Fig. 6c and d), because of this it was somewhat complicated for us to predict the shape of nanoparticles. Previously, a similar guest encapsulation associated with nanoparticle formation was found for another hydrophobic drug molecule (Saikosin, Limpaseni, & Pongsawasdi, 2002). The above results suggest that the CD may serve as delivery carrier for hydrophobic drugs. The irregularity in the size of the nano-encapsulated complexes is an essential topic to be addressed. Further, the

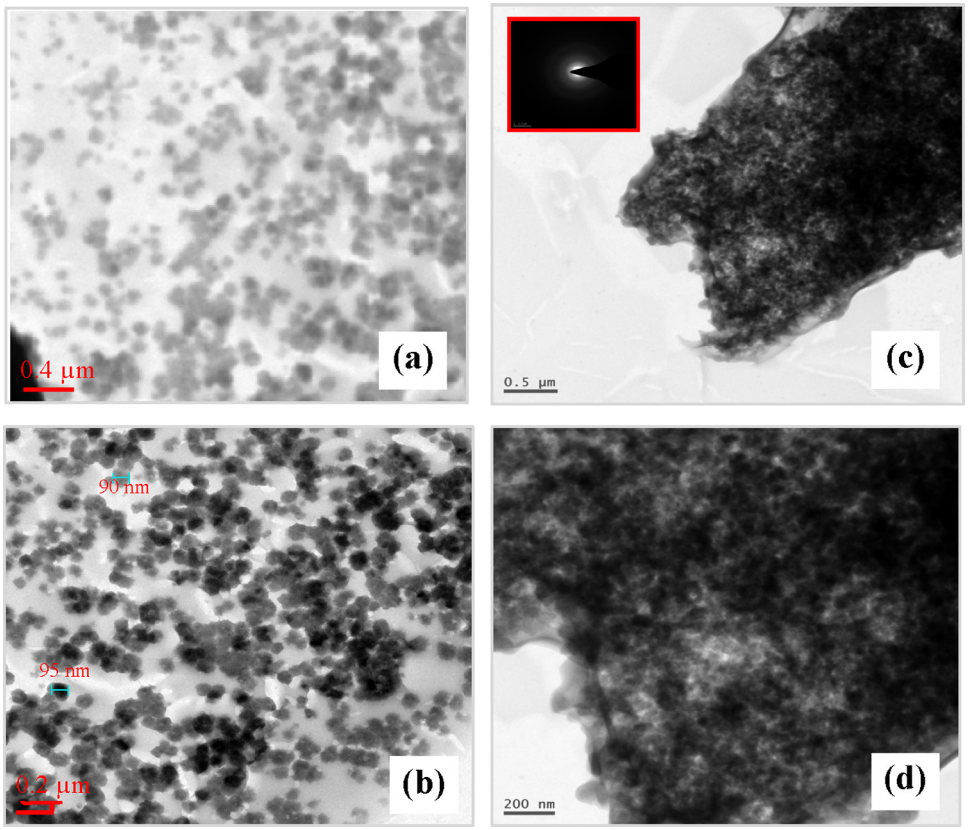

Fig. 6. TEM images of (a and b) SDMO/α-CD and (c and d) SDMO/β-CD nanoparticles. Inset in figure (c) shows SAED pattern of SDMO/β-CD complex.

manipulation of controllable nanoparticle by molecular encapsulation is a very challenging and attractive field to be focused for further study. The inset in Fig. 6c shows the selected area electron diffraction (SAED) pattern of SDMO/β-CD complex. From the SAED pattern, it is confirmed that in the complexation process of SDMO with CDs, the crystalline drug is completely transferred into amorphous nature, which is in accordance with the powder XRD results.

3.5.6. XRD analysis

Supporting evidence for the complexation of SDMO with α-CD and β-CD was also obtained from Powder X-ray diffractometry (XRD). XRD is a useful method for the detection of CD encapsulation and it has been used to assess the degree of crystallinity of the given sample. When a true complex is formed, the overall number of crystalline structure are reduced and more number of amorphous structures are increased (Wang, Cao, Sun, & Wang, 2011; Eid et al., 2011). Hence, the solid complexes exhibit less numbered as well as less intense peaks. This shows that overall crystallinity of complex is decreased and due to amorphous nature the solubility is increased. Therefore in this work, the XRD patterns for SDMO, α-CD, β-CD and the solid complexes were collected at diffraction angles (2θ) from 5° to 50° and are depicted in Fig. 7. SDMO exhibits characteristic peaks at 2θ values of 10.28°, 12.10°, 14.10°, 19.02°, 20.93°, 22.02°, 24.94°, 28.13°, 31.77°, 32.95°, 35.14° and 39.23°, indicating the high degree of crystallinity. The XRD pattern of α-CD showed characteristic peaks at 2θ values of 9.46°, 11.82°, 14.19°, 17.93°, 21.57° and 27.12°. However, the diffractogram of β-CD crystals exhibited important peaks at 2θ values of 8.95°, 10.56°, 12.46°, 18.75°, 22.57°, 27.03°, 31.86° and 34.59°. Most of the characteristic peaks of SDMO were present in the diffraction patterns of physical mixtures of the drug with CDs (Figures not shown) without loss of intensity. In contrast, the XRD patterns of the SDMO/α-CD and SDMO/β-CD complexes differed considerably from those of the drug and the CD alone with a completely diffuse diffraction pattern, which reveals the amorphous nature of the samples. The intensity of peaks at 10.28°, 14.10°, 19.02°, 20.93°, and 24.94° of SDMO were reduced significantly in SDMO/CD inclusion complex diffraction patterns which suggests reduction in crystallinity of SDMO (Fig. 7) (Siva et al., 2013). Some low intensity peaks of SDMO at 32.95°, 35.14°, 39.23° were absent after complexation with CDs. This different pattern might be due to inclusion of SDMO molecule into the cavity of CD. Further, appearance of new peaks at 2θ values for the patterns of SDMO/α-CD (12.19° and 13.19°) and SDMO/β-CD (15.29°, 24.85° and 28.22°) inclusion complex indicates the change in SDMO and CD environment after inclusion complexation.

3.6. Molecular modeling

In order to further scrutinize the mechanism of inclusion complexation between SDMO and CDs, semiempirical quantum mechanical calculations using PM3 program were performed for the most favorable inclusion modes and to obtain a meaningful three-dimensional visualization of the complex. This method is a very useful tool for investigating the CD inclusion complexes in order to calculate the binding energy as well as the geometrical structure of the inclusion complexes and it is already proved that this method is more reproducible when compared with the experimental data (Castro et al., 1996). Fig. S2 (see Supplementary data) illustrates upper and side views of the optimized structure of inclusion complexes obtained by energy minimization at PM3 level of theory. The energetic features and thermodynamic parameters (enthalpy, entropy, and free energy change) of the guest (SDMO), host (α/β-CD) and the inclusion complexes are summarized in Table 1. In the case of SDMO/α-CD complex (Fig. S2a), the conformation obtained has the SO_2—NH group oriented at the center of the cavity, while amino and methoxy groups exposed to outer side of

Table 1
Energetic features and thermodynamic parameters for SDMO, α-CD, β-CD and its 1:1 inclusion complexes obtained by PM3 method.

Properties	SDMO	α-CD	β-CD	SDMO/α-CD	SDMO/β-CD
E (kcal/mol)	−87.12	−1247.62	−1457.75	−1341.45	−1555.18
ΔE (kcal/mol)				−6.71	−10.31
H (kcal/mol)	89.47	−570.84	−667.55	−485.96	−584.01
ΔH (kcal/mol)				−4.59	−5.93
G (kcal/mol)	42.35	−676.37	−789.52	−598.46	−725.35
ΔG (kcal/mol)				35.56	21.82
S (kcal/mol-Kelvin)	0.158	0.353	0.409	0.438	0.488
ΔS (kcal/mol-Kelvin)				−0.073	−0.079

the CD cavity. The theoretical results obtained for SDMO/β-CD complex, Fig. S2b, demonstrated that the encapsulation occurs in a similar fashion to SDMO/α-CD complex. The pictures clearly pointed out the possibility for the interactions of the NH_2 or OCH_3 groups with the CD cavity. However, the orientation of these inclusion complexes adopted by this conformation is more favored. These results are well consistent with our geometry obtained by the spectral titration measurements and ^{1}H NMR results. The theoretically calculated formation energy values for these structures by PM3 method are given in Table 1 along with results for those of isolated drug and CD molecules for comparison purpose. The PM3 calculations express that the formation energy of the inclusion complex is always lower than that of the sum of the energies of the isolated drug and host molecules, suggesting SDMO formed the most favorable complexes with both CDs. The more negative magnitude of formation energy obtained for β-CD complex indicates that β-CD complex is more stable when compared to α-CD complex.

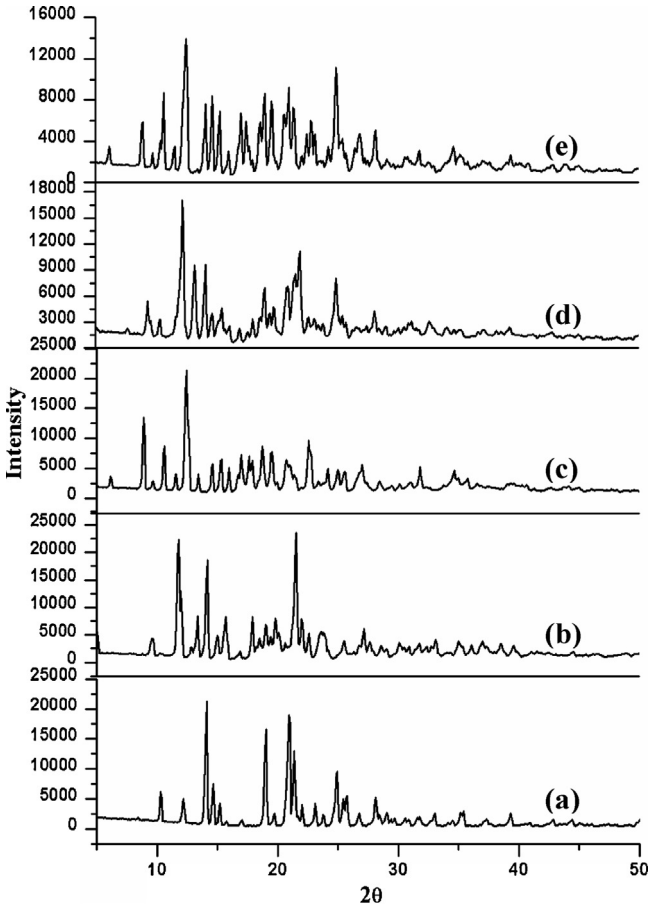

Fig. 7. Powder XRD patterns of (a) SDMO, (b) α-CD, (c) β-CD, (d) SDMO/α-CD complex and (e) SDMO/β-CD complex.

To inspect the thermodynamics of the complexation process, we carried out statistical thermodynamic calculations at 1 atm and 298.15 K by PM3 method. The thermodynamic quantities of the encapsulation process, such as binding energy (ΔE), enthalpy change (ΔH), Gibbs free energy change (ΔG) and entropy change (ΔS) were determined and the results are summarized in Table 1. In order to quantify the interaction between SDMO and CDs in the optimized geometries, we have calculated the binding energy (ΔE) for the minimum energy structures. The variation in the ΔE values indicates the nature of the driving force involved in the complexation process. More negative is the stabilization energy, more thermodynamically favorable is the formation of the inclusion complex. From Table 1, it can be observed that the negative binding energies for the inclusion complexes indicate that the encapsulation processes are thermodynamically favorable in nature. The difference in binding energies for the inclusion complexes of the drug with CDs is 3.60 kcal/mol, which suggests that the SDMO/β-CD complex is more stable than that of α-CD complex.

It is observed from the results that the complexation reactions of SDMO with CDs were exothermic, which was judged from the negative ΔE and ΔH values. The negative binding energy and enthalpy changes suggested that the inclusion processes were energetically and enthalpically favorable in nature. Further, the ΔH value for the encapsulation complex of SDMO with β-CD is more negative indicating strong interactions between SDMO and CD cavity in this orientation. The theoretical ΔG values were different from our earlier experimental findings. The theoretically calculated Gibbs free energy changes (ΔG) using PM3 calculations are found with positive magnitude, suggesting that the inclusion reaction was a non-spontaneous process. The difference in ΔG values can be explained by the solvent effect. The actual experiments were conducted in aqueous medium but the computational work was done at vacuum phase. Unfortunately, because of limitations in the calculating ability of our computer and the large molecular size of CD, the statistical thermodynamic calculations for these systems could not be performed in aqueous phase as well as in excited state. However, it was observed that the solvent effect on the host-guest interactions easily changes the inclusion process from a non-spontaneous process in the gas phase to a spontaneous one in the aqueous phase. The host-guest interaction causes an enthalpy–entropy compensating process in the gas phase whereas the same interaction causes an enthalpy–entropy codriven process in aqueous solution, because inclusion complexation releases a number of water molecules from the cavities of CD. However, the PM3 results are in good agreement with that of experimental results.

4. Conclusions

The inclusion complexation behavior of SDMO with α-CD and β-CD have been investigated by absorption, fluorescence, time-resolved fluorescence, ^{1}H NMR, FTIR, DSC, SEM, TEM, XRD and molecular modeling methods. The association constant of inclusion

complexes was determined and 1:1 stoichiometry was confirmed by Benesi–Hildebrand double reciprocal plots. Nanosecond time-resolved studies indicated that SDMO exhibits biexponential decay in water whereas triexponential decay in CD as a consequence of complex formation. The application of FT-IR spectroscopy allowed the physicochemical characterization of physical mixtures and solid inclusion complexes. The inclusion complexes showed differences in spectroscopic profiles when compared to free SDMO and CDs, and the physical mixtures showed a simple combination of these substances. The results obtained from ^{1}H NMR, FT-IR, DSC, SEM, TEM and XRD studies confirmed that the formation of inclusion complexes in solid state. TEM examinations revealed that the nano-sized particles could be produced from the molecular encapsulation of SDMO within the CD cavity. Both experimental and molecular modeling methods proved that the drug was partially included in the CD cavity with aniline moiety located nearer at primary rim and the pyrimidine ring nearer at secondary rim. Thermodynamic parameters (ΔG, ΔH and ΔS) suggested that the inclusion complex formation is an enthalpy driven process and the driving force governing the complexation process is van der Waals interactions.

Acknowledgements

This work is supported by the CSIR [No. 01(2549)/12/EMR-II] and UGC [F. No. 41-351/2012(SR)] New Delhi, India. One of the authors S. Siva is thankful to UGC-RGNF, New Delhi for the award of SRF (No. F.16-1281(SC)/2009(SA-III)). We are grateful to Dr. R. Chandrasekar, Associate Professor for his kind help and UGC Networking Resource Center, School of Chemistry, UoH for providing instrumental facilities.

Appendix A. Supplementary data

Supplementary data associated with this article can be found, in the online version, at http://dx.doi.org/10.1016/j.carbpol.2013.10.016.

References

Benesi, A., & Hildebrand, J. H. (1949). A spectrophotometric investigation of the interaction of iodine with aromatic hydrocarbons. *Journal of American Chemical Society*, *71*, 2703–2707.

Carrier, R. L., Miller, L. A., & Ahmed, I. J. (2007). The utility of cyclodextrins for enhancing oral bioavailability. *Journal of Controlled Release*, *123*, 78–99.

Castro, R., Berardi, M. J., Cordova, E., de Olza, M. O., Kaifer, A. E., & Evanseck, J. D. (1996). Unexpected roles of guest polarizability and maximum hardness, and of host solvation in supramolecular inclusion complexes: A dual theoretical and experimental study. *Journal of American Chemical Society*, *118*, 10257–10268.

Chung, H.-H., Lee, J.-B., Chung, Y.-H., & Lee, K.-G. (2009). Analysis of sulfonamide and quinolone antibiotic residues in Korean milk using microbial assays and high performance liquid chromatography. *Food Chemistry*, *113*, 297–301.

Connors, K. A. (1997). The stability of cyclodextrin complexes in solution. *Chemical Reviews*, *97*, 1325–1357.

Delrivo, A., Zoppi, A., & Longhi, M. R. (2012). Interaction of sulfadiazine with cyclodextrins in aqueous solution and solid state. *Carbohydrate Polymers*, *87*, 1980–1988.

Eid, E. E. M., Abdul, A. B., Suliman, F. E. O., Sukari, M. A., Rasedee, A., & Fatah, S. S. (2011). Characterization of the inclusion complex of zerumbone with hydroxypropyl-β-cyclodextrin. *Carbohydrate Polymers*, *83*, 1707–1714.

Fernandez, L., Martinez-Oharriz, M. C., Martin, C., Velaz, I., Sanchez, M., & Zornoza, A. (2008). Analysis of the complexation of gemfibrozil with γ- and hydroxypropyl-γ-cyclodextrins. *Journal of Pharmaceutical and Biomedical Analysis*, *47*, 943–948.

Garnero, C., Aiassa, V., & Longhi, M. R. (2012). Sulfamethoxazole:hydroxypropyl-β-cyclodextrin complex: Preparation and characterization. *Journal of Pharmaceutical and Biomedical Analysis*, *63*, 74–79.

Hadaruga, N. G., Hadaruga, D. I., Paunescu, V., Tatu, C., Ordodi, V. L., Bandur, G., et al. (2006). Thermal stability of the linoleic acid/α- and β-cyclodextrin complexes. *Food Chemistry*, *99*, 500–508.

Inoue, Y., Hakushi, T., Liu, Y., Tong, L. H., Shen, B. J., & Jin, D. S. (1993). Thermodynamics of molecular recognition by cyclodextrins. 1. Calorimetric titration of inclusion complexation of naphthalenesulfonates with alpha-, beta-, and gamma-cyclodextrins: Enthalpy–entropy compensation. *Journal of American Chemical Society*, *115*, 475–481.

Kacso, I., Borodi, Gh., Farcas, S. I., Hernanz, A., & Bratu, I. (2010). Host-guest system of vitamin B10 in beta-cyclodextrin: Characterization of the interaction in solution and in solid state. *Journal of Inclusion Phenomena and Macrocyclic Chemistry*, *68*, 175–182.

Kishida, K., & Furusawa, N. (2005). Simultaneous determination of sulfamonomethoxine, sulfadimethoxine, and their hydroxy/N4-acetyl metabolites with gradient liquid chromatography in chicken plasma, tissues, and eggs. *Talanta*, *67*, 54–58.

Lehman, J., & Klienpeter, E. (1991). 1H NMR spectroscopy as a probe of intermolecular interactions in β-cyclodextrin inclusion compounds. *Journal of Inclusion Phenomena and Macrocyclic Chemistry*, *10*, 233–239.

Li, G., & Mcgown, L. B. (1994). Molecular nanotube aggregates of beta- and gama-cyclodextrins linked by diphenylhexatrienes. *Science*, *264*, 249–251.

Loftsson, T., & Duchene, D. (2007). Cyclodextrins and their pharmaceutical applications. *International Journal of Pharmaceutics*, *329*, 1–11.

Perez-Trallero, E., & Iglesias, L. (2003). Tetraciclinas, sulfamidas y metronidazol. *Enfermedades Infecciosas y Microbiología Clínica*, *21*, 520–529.

Prabhu, A. A. M., Sankaranarayanan, R. K., Venkatesh, G., & Rajendiran, N. (2012). Dual fluorescence of fast blue rr and fast violet B: Effects of solvents and cyclodextrin complexation. *Journal of Physical Chemistry B*, *116*, 9061–9074.

Prabhu, A. A. M., Venkatesh, G., & Rajendiran, N. (2010). Spectral characteristics of sulfa drugs: Effect of solvents, pH and β-cyclodextrin. *Journal of Solution Chemistry*, *39*, 1061–1086.

Premakumari, J., Allan Gnana Roy, G., Prabhu, A. A. M., Venkatesh, G., Subramanian, V. K., & Rajendiran, N. (2011). Spectral characteristics of sulphadiazine, sulphisomidine: Effect of solvents, pH and β-cyclodextrin. *Physics and Chemistry of Liquids*, *49*, 108–132.

Saikosin, R., Limpaseni, T., & Pongsawasdi, P. (2002). Formation of inclusion complexes between cyclodextrins and carbaryl and characterization of the complexes. *Journal of Inclusion Phenomena and Macrocyclic Chemistry*, *44*, 191–196.

Schmitt, H., Haapakangas, H., & van Beelen, P. (2005). Effects of antibiotics on soil microorganisms: Time and nutrients influence pollution-induced community tolerance. *Soil Biology and Biochemistry*, *37*, 1882–1892.

Siva, S., Thulasidhasan, J., & Rajendiran, N. (2013). Host-guest inclusion complex of propafenone hydrochloride with α- and β-cyclodextrins: Spectral and molecular modeling studies. *Spectrochimica Acta Part A: Molecular and Biomolecular Spectroscopy*, *115*, 559–567.

Sivasankar, T., Prabhu, A. A. M., Karthick, M., & Rajendiran, N. (2012). Encapsulation of vanillylamine by native and modified cyclodextrins: Spectral and computational studies. *Journal of Molecular Structure*, *1028*, 57–67.

Sun, T., Zhang, H., Kong, L., Qiao, H., Li, Y., Xin, F., et al. (2011). Controlled transformation from nanorods to vesicles induced by cyclomaltoheptaoses (β-cyclodextrins). *Carbohydrate Research*, *346*, 285–293.

Szejtli, J. (1998). Introduction and general overview of cyclodextrin chemistry. *Chemical Reviews*, *98*, 1743–1753.

Ulusoy, T., Topacli, A., & Ide, S. (1998). Spectroscopic and structural studies on Ni-sulfadimethoxine complex. *Pharmaceutica Acta Helvetiae*, *72*, 295–300.

Venkatesh, G., Sivasankar, T., Karthick, M., & Rajendiran, N. (2013). Inclusion complexes of sulphanilamide drugs and β-cyclodextrin: A theoretical approach. *Journal of Inclusion Phenomena and Macrocyclic Chemistry*, http://dx.doi.org/10.1007/s10847-012-0248-z

Wang, J., Cao, Y., Sun, B., & Wang, C. (2011). Physicochemical and release characterisation of garlic oil-β-cyclodextrin inclusion complexes. *Food Chemistry*, *127*, 1680–1685.

Yu, T.-H., Lin, A. Y., Panchangam, S. C.-C., Andy Hong, P.-K., Yang, P.-Y., & Lin, C.-F. (2011). Biodegradation and bio-sorption of antibiotics and non-steroidal anti-inflammatory drugs using immobilized cell process. *Chemosphere*, *84*, 1216–1222.